Spectroscopy of $Y_3Al_5O_{12}:Nd^{3+}$ under high-power, picosecond-pulse excitation

George E. Venikouas, Greg J. Quarles, John P. King,* and Richard C. Powell
Department of Physics, Oklahoma State University, Stillwater, Oklahoma 74078
(Received 7 March 1984)

High-power, picosecond-pulse excitation was used to study the dynamics of the pumping and decay processes in $Y_3Al_5O_{12}:Nd^{3+}$. The observed fluorescence spectral lines are assigned to transitions from three different metastable states excited by both single-photon and two-photon absorption. The branching ratios, lifetimes, and quantum efficiencies of the metastable states are obtained from the data as well as the two-photon absorption cross sections. The results provide useful information concerning ultraviolet pumping efficiencies of the Nd-YAG (Nd-doped yttrium aluminum garnet) laser transition and the $5d$-$4f$ nonradiative decay rate for this material. In addition, the time-resolved spectroscopy method employed here is shown to be an extremely sensitive technique for obtaining two-photon absorption cross sections.

I. INTRODUCTION

Despite the importance of $Y_3Al_5O_{12}:Nd^{3+}$ (Nd-YAG) as a solid-state laser material, there are still some aspects of its spectroscopic properties which are not well characterized.[1] One area in which very little work has been done is in studying the pumping and relaxation dynamics of the higher-energy electronic states of the Nd^{3+} ion.[2–4] These states can be reached by ultraviolet, x-ray, electron-beam, or high-power multiphoton visible laser excitation. For some specific applications, these pumping sources may be preferable to the standard visible flashlamp pumping and thus it is important to understand the spectral dynamics of these upper energy levels.

We report here the results of an investigation of the spectroscopic properties of a Nd-YAG crystal after excitation by high-power picosecond pulses from the various harmonics of a Nd-YAG laser. The time-resolved fluorescence spectra, fluorescence lifetimes, and rise times were measured as a function of laser power for frequency-doubled, -tripled, and -quadrupled Nd-YAG laser lines. The results are consistent with emission from three metastable states after single-photon and two-photon pumping. Models are proposed to describe the observed spectral dynamics, and comparing their predictions to the experimental results provides information such as the quantum efficiencies and branching ratios for the metastable states as well as the two-photon absorption cross sections. The results provide the first measured value for the $5d$-$4f$ radiationless decay rate for this system. In addition, it is shown that the time-resolved spectroscopy technique employed here is a very sensitive way to determine two-photon cross sections.

II. EXPERIMENTAL PROCEDURE

A block diagram of the experimental setup is shown in Fig. 1. A passively mode-locked, Nd-YAG oscillator provides a train of pulses and a pulse-switching network selects a single pulse from the train. This is sent through an amplifier resulting in a pulse of about 30 ps in duration and 25 mJ energy. Frequency-doubling, -tripling, or -quadrupling crystals are used to obtain the desired wavelength for sample excitation.

The sample investigated was cut from a commercial laser rod and contained 0.87 at.% Nd^{3+}. The quantum efficiency of the $^4F_{3/2}$ level was previously measured to be about 60%.[5]

The sample fluorescence is analyzed by a $\frac{1}{4}$-m monochromator and detected by an RCA C31034 photomultiplier tube. The signal is processed by a boxcar integrator triggered by the laser to obtain time-resolved spectra. The signal-to-noise ratio is improved by a signal averager before the results are displayed on a chart recorder. A beam splitter picks off part of the pulse to monitor the shot-to-shot intensity variation of the laser.

The energy levels of the $4f^3$ electronic configuration of Nd^{3+} are shown in Fig. 2. Additional states belonging to

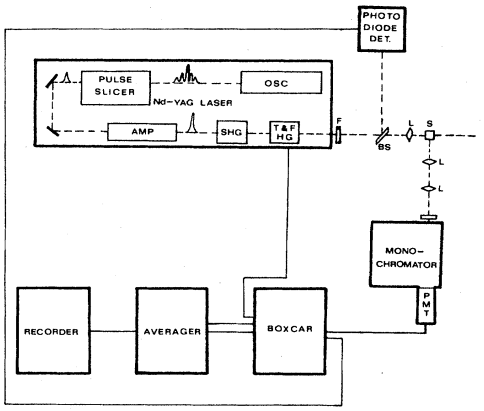

FIG. 1. Experimental apparatus for high-power, picosecond-pulse excitation experiments. The laser is a passively mode-locked Nd-YAG system with a single-stage amplifier and frequency-doubling, -tripling, and -quadrupling crystals. *F*, filter; BS, beam splitter; *L*, lens *S*, sample.

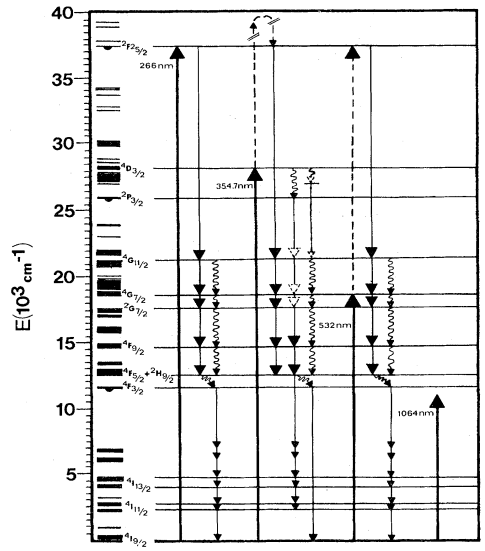

FIG. 2. Energy levels of the $4f^3$ configuration of Nd^{3+} with important multiplets labeled, approximate crystal-field splittings indicated by linewidths, and the observed metastable states in YAG indicated as semicircles. (The highest metastable state is referred to as either $^2(F\,2)_{5/2}$ or $\beta^2F_{5/2}$ in the literature;[2,3] we have arbitrarily chosen to use the former notation.) The important absorption and emission transitions for the different excitation wavelengths used in this work are also shown. The solid arrows with straight shafts represent radiative transitions, and those with dashed shafts represent two-photon transitions; the wavy shafts represent radiationless transitions. Arrows with open heads represent infrared transitions which are implied but not directly observed in this work.

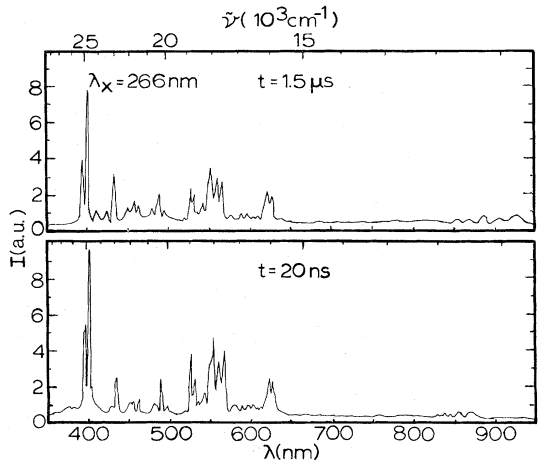

FIG. 3. Fluorescence spectra of Nd-YAG at two times after the excitation pulse at 266 nm.

the $4f^25d$ configuration are found at higher energy beginning at about 40 000 cm^{-1}. Typical spectroscopic studies have involved excitation in the visible region of the spectrum, resulting in fast radiationless relaxation to the $^4F_{3/2}$ metastable state after which fluorescence emission occurs in the near-infrared spectral region. The four Nd-YAG—laser harmonic lines used for pumping are shown in the figure. Attempts to excite fluorescence with multiphoton absorption of the primary 1064-nm radiation were unsuccessful. The doubled output at 532 nm resulted in single-photon absorption in the $^4G_{7/2}$ level and two-photon absorption to the $^2(F\,2)_{5/2}$ level[2,3] (or $\beta^2F_{5/2}$). The tripled output at 354.7 nm gives single-photon absorption in the $^4D_{3/2}$ level and two-photon absorption in the $5d$ levels. The quadrupled output at 266 nm results in single-photon absorption in the $^2(F2)_{5/2}$ level and no observed two-photon absorption. The properties of the fluorescence emission observed after these different types of pumping are discussed in the following sections.

III. RESULTS FOR 266-nm PUMPING

Figure 3 shows the fluorescence spectra obtained at two times after the excitation pulse for quadrupled Nd-YAG—laser pumping at 266 nm. For this excitation wavelength, the emission intensity of all of the lines in the spectrum are found to vary linearly with pump power, indicating that single-photon absorption is responsible for exciting all of these transitions. The spectral lines can be divided into two distinct groups according to their lifetimes as seen by the spectra recorded at two different times after the pulse as shown in Fig. 3. These are associated with fluorescence emission transitions from two dif-

TABLE I. Characteristics of metastable states in Nd-YAG.

Parameter	State $^4F_{3/2}$	$^2P_{3/2}$	$^2(F\,2)_{5/2}$
τ_f (μs)	220	0.32	3.02
η	0.60	0.96	0.99
ΔE (cm^{-1})	4600	2150	3400
B_i	$^4I_{9/2}$: 0.366	$^4I_{11/2}$: 2.4×10^{-4}	$^4F_{5/2}$: 0.23[a]
	$^4I_{11/2}$: 0.500	$^4I_{13/2}$: 1.44×10^{-4}	$^4F_{9/2}$: 0.03
	$^4I_{13/2}$: 0.130	$^4F_{5/2}$: 1.36×10^{-4}	$^2G_{7/2}$ 0.03
	$^4I_{15/2}$: 0.004	$^4F_{9/2}$: 2.8×10^{-4}	$^4G_{7/2}$: 0.43
		ir: 0.9992	$^4G_{11/2}$: 0.28

[a]Also includes transitions to the $^2H_{9/2}$ levels.

ferent metastable states. Figure 2 shows that this excitation wavelength directly pumps the $^2(F2)_{5/2}$ level. The lines appearing in the fluorescence spectrum with a lifetime of 3.02 μs are associated with transitions from this level to the various crystal-field-split components of the $^4G_{11/2}$, $^4G_{7/2}$, $^2G_{7/2}$, $^4F_{9/2}$, and $^4F_{5/2}+^2H_{9/2}$ multiplets after which fast radiationless decay occurs to the $^4F_{3/2}$ level. This is followed by the well-known near-infrared emission transitions having a lifetime of 220 μs.

Thus from the time-resolved spectra after 266-nm excitation, the $^2(F2)_{5/2}$ level is identified as a second metastable state for Nd^{3+} emission in YAG crystals. The branching ratios for the emission transitions from this level to the different terminal multiplets are given by

$$B_i = \sum_j I_{ij} \Big/ \sum_{i,j} I_{ij} \ , \tag{1}$$

where i represents the different free-ion—term values and j represents the different crystal-field components within each term. The branching ratios for this upper metastable state are found from the spectra shown in Fig. 3 and listed in Table I.

The time evolution of the spectra shown in Fig. 3 can be described by the simplified rate model shown in Fig. 4. n_1 and n_3 represent the concentration of ions in excited states $^4F_{3/2}$ and $^2(F2)_{5/2}$, respectively, β_1 and β_3 are the fluorescence decay rates of these levels, and W_3 is the pumping rate for the upper metastable state. The rate equations describing the time evolution of the excited state populations are

$$\frac{dn_1}{dt} = \beta_3 n_3 - \beta_1 n_1 \ , \tag{2}$$

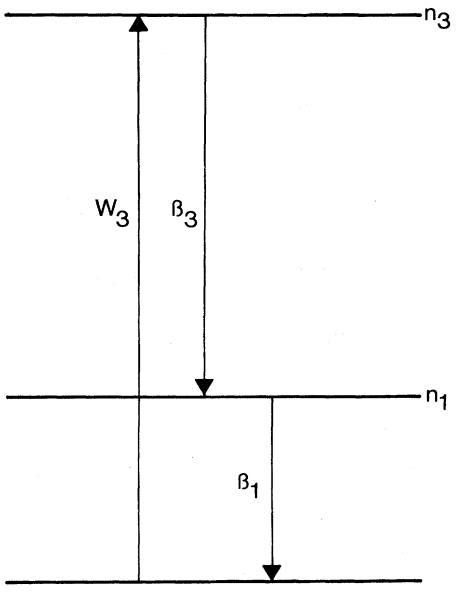

FIG. 4. Model for explaining observed spectral dynamics after 266-nm excitation. See text for definition of parameters.

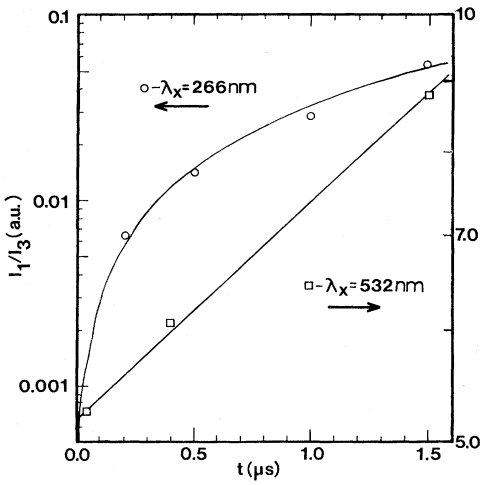

FIG. 5. Time evolution of the ratios of the integrated fluorescence intensities of the emission from the $^4F_{3/2}$ and $^2(F2)_{5/2}$ metastable states after 266- and 532-nm excitations. See text for explanation of the theoretical line.

$$\frac{dn_3}{dt} = W_3 - \beta_3 n_3 \ . \tag{3}$$

The basic assumptions of this model are that the $^4F_{3/2}$ level is pumped only through relaxation from the $^2(F2)_{5/2}$ level and that the latter level has 100% quantum efficiency and has no radiative transitions that bypass the former level and terminate on levels of the ground-state term or that result in unobserved infrared radiation. The solutions of Eqs. (2) and (3) for δ-function excitation can be related to the measured relative fluorescence intensity ratios through

$$I_1(t)/I_3(t) = K[\beta_3/(\beta_3-\beta_1)]\{\exp[(\beta_3-\beta_1)t]-1\} \ , \tag{4}$$

where $k = \beta_1^r B_1/\beta_3^r$. Here, the β_i^r are the radiative decay rates of the two metastable states and B_1 is the branching ratio for the transitions from the lower metastable state to the $^4I_{9/2}$ ground-state levels. Figure 5 shows the ratios of the integrated fluorescence intensities of all of the $^2(F2)_{5/2}$ transitions and the visible transitions from the $^4F_{3/2}$ level shown in Fig. 3. The solid line represents the prediction of Eq. (4) with no adjustable parameters. The excellent fit between theory and experiment indicates that the assumptions underlying the simplified model used here are justified for this case.

IV. RESULTS FOR 532-nm PUMPING

Figure 6 shows the fluorescence spectra at two times after the laser excitation pulse for doubled Nd-YAG pumping at 532 nm. The same lines appear in the spectra as seen in Fig. 3, but their relative intensities are different and change with pumping power. As an example of this, Fig. 7 shows the change in the integrated fluorescence intensity of the major emission line at 402 nm as a function of excitation-pulse energy. The observed quadratic depen-

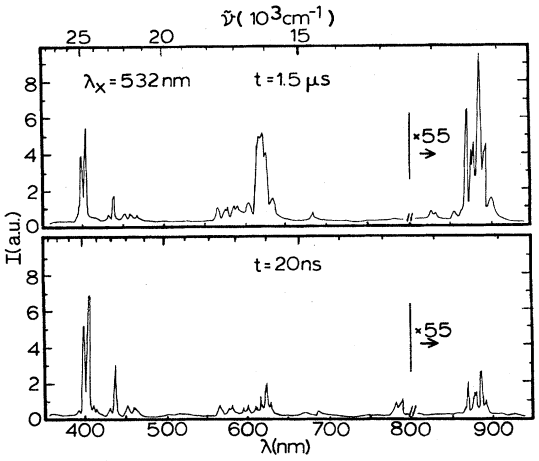

FIG. 6. Fluorescence spectra of Nd-YAG at two times after the excitation pulse at 532 nm.

dence indicates that this excitation wavelength results in two-photon absorption terminating on the $^2(F2)_{5/2}$ metastable state. The fluorescence from this level is the same as that discussed in the preceding section following single-photon pumping. As seen in Fig. 2, the intermediate state for this two-photon transition is the $^4G_{7/2}$ level, which is directly pumped through one-photon absorption processes. Only part of the ions excited to this intermediate state undergo two-photon excitation, while the rest decay radiationlessly to the $^4F_{3/2}$ metastable state from which the standard emission transitions occur.

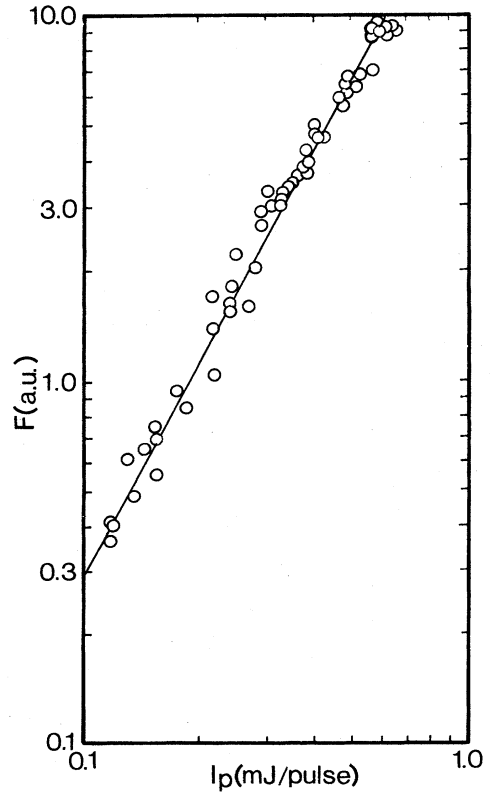

FIG. 7. Integrated fluorescence intensity of the 402-nm spectral line as a function of laser power at 532-nm excitation.

The excited-state dynamics for this case can be described by a simplified rate model similar to that shown in Fig. 4, but with an additional parameter W_1 to describe the single-photon pumping rate of the $^4F_{3/2}$ metastable state through fast radiationless relaxation from the $^4G_{7/2}$ level and with the two-photon pumping rate of the $^2(F2)_{5/2}$ metastable state given by W_3'. The rate equations for this model are

$$\frac{dn_1}{dt}=W_1+\beta_3 n_3-\beta_1 n_1 , \tag{5}$$

$$\frac{dn_3}{dt}=W_3'-\beta_3 n_3 . \tag{6}$$

The basic assumption of this model is that the cascade nonradiative decay processes from the $^4G_{7/2}$ state to the $^4F_{3/2}$ state are very fast and efficient. The ratios of the fluorescence intensities can be obtained from the solutions of Eqs. (5) and (6) as

$$\frac{I_1(t)}{I_3(t)}=[I_1(0)/I_3(0)]\exp[(\beta_3-\beta_1)t] +K[\beta_3/(\beta_3-\beta_1)]\{\exp[(\beta_3-\beta_1)t]-1\} . \tag{7}$$

Figure 5 shows the ratios of the integrated fluorescence intensities of the two metastable states at three times after the excitation pulse for a specific level of laser power. The solid line in the figure represents the best fit to the data using Eq. (7) and treating the ratio of the initial intensities as an adjustable parameter. The excellent fit between theory and experiment indicates the validity of the proposed model and gives the value of $I_1(0)/I_3(0)$ listed in Table II.

The two-photon absorption cross section can be derived from these results through the expression

$$\frac{I_1(0)/\hbar\omega_1}{I_3(0)/\hbar\omega_3}=\frac{\beta_1^r n_1(0)}{\beta_3^r n_3(0)} =\frac{\beta_1^r\sigma_1' I_p n_0 L}{\beta_3^r I_p^2\sigma_3^{(2)} n_0 L} =(\beta_1^r/\beta_3^r)(\sigma_1'/\sigma_3^{(2)})(1/I_p) , \tag{8}$$

where I_p is the intensity of the laser pulse, σ_1' and $\sigma_3^{(2)}$ are the relevant one- and two-photon absorption cross sections, n_0 represents the total concentration of Nd^{3+} ions, L is the sample thickness, and $\hbar\omega_i$ is the average energy of the photons emitted from the ith metastable state. Using the radiative decay rates determined from the information listed in Table I, the measured value for the fluorescence intensity ratio at an excitation power level of $I_p=1.38\times10^{28}$ photons/cm^2 s^{-1}, and the value for the absorption cross section of the $^4G_{7/2}$ level from Ref. 6 gives a value of

$$\sigma_3^{(2)}=3.12\times10^{-55}\ \text{cm}^4\,\text{s/(photon ion)} .$$

TABLE II. Summary of results.

Parameter	Experimental	Theoretical
τ_d^{-1} (s^{-1})	5.00×10^{8}	
W_{nr}^{p} (s^{-1}): $^2P_{3/2}$		1.38×10^{5}
$^2F2_{5/2}$		3.05×10^{3}
$\sigma^{(2)}$ [cm^4 s/(photon ion)]: $^2F2_{5/2}$	3.21×10^{-55}	1.64×10^{-56}
$5d$[a]	1.27×10^{-49}	3.69×10^{-56}
$I_1(0)/I_3(0)$ ($\lambda_x=532$ nm)[b]	51.6	
$I_2(0)/I_3(0)$ ($\lambda_x=354.7$ nm)[b]	3.69	
K'	1.058	

[a]Nature of the final states is unknown and may be a high-energy $4f$ level.
[b]These values are normalized for photon energies and $I_1(0)$ is corrected for the branching ratio of the observed fraction of the transitions from this level.

V. RESULTS FOR 354.7-nm PUMPING

Figure 8 shows the fluorescence spectra at two times after the laser pulse for tripled Nd-YAG excitation at 354.7 nm. These spectra contain the same lines as seen in Figs. 3 and 6 as well as numerous additional lines. The new lines all exhibit a faster lifetime of about 0.32 μs. The relevant transitions for this pumping wavelength are shown in Fig. 2. The $^4D_{3/2}$ level is directly excited by the laser pulse. Some of the excited ions undergo rapid radiationless relaxation to the $^2P_{3/2}$ level, while the rest of the ions undergo two-photon excitation to the $5d$ levels. After the latter process, radiationless decay back to the $^2(F2)_{5/2}$ metastable state occurs followed by the emission processes discussed in the preceding sections. After the former process the $^2P_{3/2}$ level acts as a new metastable state resulting in the transitions shown in Fig. 2. One important aspect of these new transitions is that only part of them terminate on levels above the $^4F_{3/2}$ level to give fluorescence from this metastable state while the remainder of the transitions go past this level and terminate on various components of the ground state term.

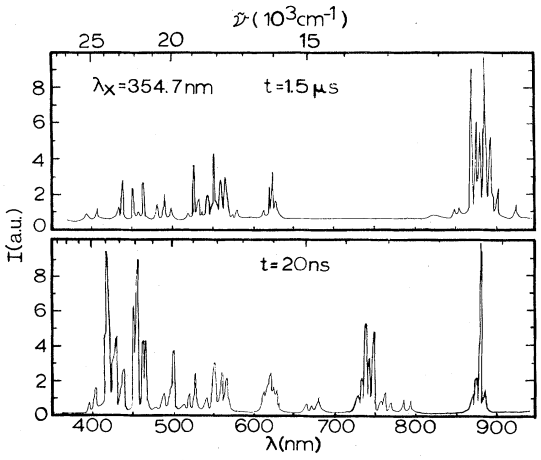

FIG. 8. Fluorescence spectra of Nd-YAG at two times after the excitation pulse at 354.7 nm.

The determination of the branching of these different types of transitions is difficult because of the possible existence of transitions emitting in the infrared spectral region (shown as dashed lines in Fig. 2).

The simplified transition rate model shown in Fig. 9 can be used to describe the excited-state dynamics for this type of pumping. In this case, three rate equations are necessary:

$$\frac{dn_1}{dt}=\beta_3 n_3+\beta_{21}n_2-\beta_1 n_1\ , \tag{9}$$

$$\frac{dn_2}{dt}=W_2-\beta_2 n_2\ , \tag{10}$$

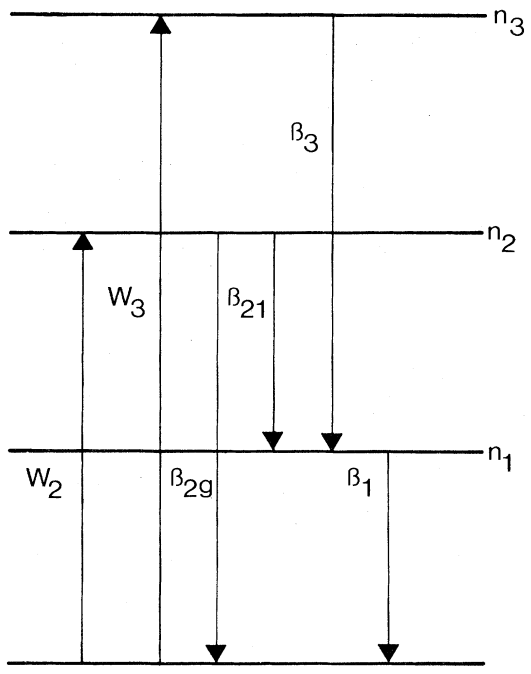

FIG. 9. Model for explaining observed spectral dynamics after 354.7-nm excitation. See text for definition of the parameters.

$$\frac{dn_3}{dt}=W_3''-\beta_3 n_3 \ . \tag{11}$$

Here W_3'' represents the two-photon pumping rate of the $^2(F2)_{5/2}$ level through radiationless relaxation from the $5d$ levels and W_2 is the rate of pumping of the $^2P_{3/2}$ level by transitions from the $^4D_{3/2}$ level. The solutions to these equations can be related to two different sets of fluorescence intensity ratios as

$$I_2(t)/I_3(t)=[I_2(0)/I_3(0)]\exp[(\beta_3-\beta_2)t] \ , \tag{12}$$

$$\begin{aligned} I_1(t)/I_2(t)=&\,[I_1(0)/I_2(0)]\exp[(\beta_2-\beta_1)t] \\ &+[I_3(0)/I_2(0)]\{K\beta_3/[(\beta_3-\beta_1)(B_{2g}+B_{21})]\}\{\exp[(\beta_2-\beta_1)t]-\exp[(\beta_2-\beta_3)t]\} \\ &+\{\beta_1' B_1 K'/[(\beta_2-\beta_1)(B_{2g}+B_{21})]\}\{\exp[(\beta_2-\beta_1)t]-1\} \ , \end{aligned} \tag{13}$$

where $K'=B_{21}+B_{21}'+W_2^{\rm nr}/\beta_2'$. Here, the branching ratios B_{21} and B_{21}' refer to the visible and infrared transitions, respectively, while $W_2^{\rm nr}$ represents the radiationless decay rate of the $^2P_{3/2}$ metastable state.

Figure 10 shows the measured values of the relevant ratios of the two different sets of integrated fluorescence intensities at three times after the excitation pulse for a specific value of laser intensity. The lines in the figure represent the best fits to the data obtained from Eqs. (12) and (13) treating the initial fluorescence intensity ratios and K' as adjustable parameters. The excellent fits to the data indicate that the model proposed here is valid. The fitting parameters are given in Table II.

Equation (8) can again be used to determine a value for the relevant two-photon absorption cross sections. In this case $I_p=1.3\times10^{27}$ photons/cm^2 s^{-1} and the value for the absorption cross section of the $^4D_{3/2}$ level is found from Ref. 6. Using the measured initial ratio of the fluorescence intensities gives $\sigma_2^{(2)}=1.27\times10^{-49}$ cm^4 s/(photon ion).

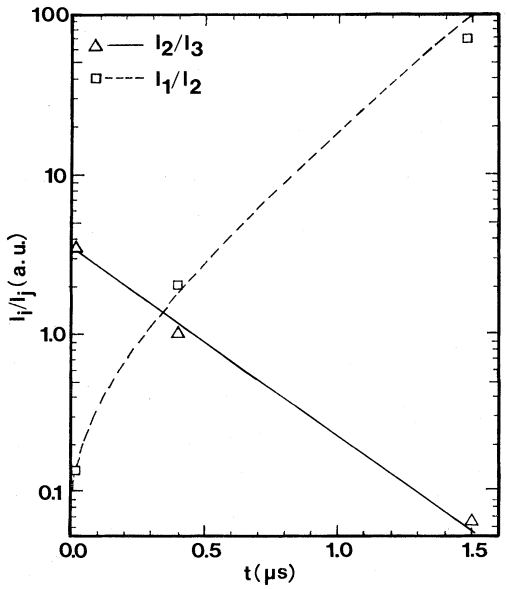

FIG. 10. Time evolution of the ratios of the fluorescence intensities of the emission from the three metastable states populated by 354.7-nm excitation. See text for explanation of the theoretical lines.

One aspect of the data which is not treated by the model discussed above is the observed rise time of approximately 15 ns of the fluorescence from the $^2(F2)_{5/2}$ level. This does not affect the time-resolved spectroscopy model because of the very different time regime involved. However, this rise time is not observed for the other two pumping wavelengths and thus it can be associated with the nonradiative decay processes from the $5d$ levels to the $4f$ levels. In a simple three-level—system model the rise time is given by[7]

$$t_m=\tau_3\tau_d\ln(\tau_d/\tau_3)/(\tau_d-\tau_3) \ , \tag{14}$$

where τ_d is the decay time of the $5d$ level. Using the measured values for the fluorescence rise time and decay time for the $^2(F2)_{5/2}$ level gives $\tau_d^{-1}\approx5\times10^8$s^{-1}.

VI. DISCUSSION AND CONCLUSIONS

The use of high-power, picosecond-pulse excitation from the various harmonics of a Nd-YAG laser has provided new information concerning the spectral dynamics of Nd^{3+} ions in YAG crystals as presented in the preceding sections. The important results of this work can be divided into three categories: characteristics of new spectral transitions, measurements of radiationless decay processes, and measurements of two-photon absorption cross sections. Each of these is discussed below.

A. New spectral transitions

The high-power, picosecond-pulse excitation at several wavelengths coupled with the time-resolved spectroscopy measurement technique employed here, shows that fluorescence emission lines from Nd^{3+} ions in YAG crystals occur throughout the visible and near-uv region of the spectrum as well as in the near-infrared region as usually reported. These lines can be associated with the transitions from three metastable states as shown in Fig. 2, the properties of which are summarized in Tables I and II.

Spectral lines similar to those reported here have been observed previously through our excitation mechanisms.[2–4] X-ray excitation[3] creates free electrons which become bound excitons at lattice-defect sites and can transfer their energy to the Nd^{3+} ions. The spectral lines obtained in this way have been interpreted in terms of transitions from the $^2(F2)_{5/2}$ level to almost all of the

lower-lying levels, including those of the ground-state term. The transition assignments of the lines given here is somewhat different than that proposed previously.[3] One major difference occurs in the uv region of the spectrum where no transitions were observed with Nd-YAG—laser excitation, but where several transitions were observed with x-ray excitation and interpreted as fluorescence originating on the $^2(F2)_{5/2}$ level and terminating on the various multiplets of the ^4I_J term. It is not clear at the present time why this difference occurs.

Similar spectral lines were also observed using nitrogen-laser-pumped dye-laser excitation in the spectral region around 590 nm.[2] The results were interpreted in terms of three-photon excitation of the $5d$ level followed by nonradiative relaxation to the $4f$ levels and fluorescence emission from the $^2(F2)_{5/2}$ metastable state. The fluorescence lifetime of these transitions was found to be about 3 μs, where is in agreement with the result reported here. Only extremely weak emission lines were observed in the 300-nm region of the spectrum which is consistent with the results reported here and again shows an interesting difference between multiphoton laser excitation and x-ray excitation.

One important result of this work is to clarify the possibility of pumping Nd-YAG lasers in the near-uv spectral region. Pumping at energies of 37 500 cm^{-1} or greater leads to very efficient excitation of the $^4F_{3/2}$ lasing metastable state through fluorescence from the $^2(F2)_{5/2}$ metastable state. Pumping in the region between 26 000 and 37 500 cm^{-1} results in emission from the $^2P_{3/2}$ metastable state. The determination of the branching ratios and quantum efficiency for this level are discussed in the next section and the results are listed in Table I. These results indicate that pumping in this intermediate metastable state still leads to efficiently populating the lasing metastable state. Further work needs to be done to correlate these results with those on x-ray and electron excitation of rare-earth ions in YAG.[3,8]

B. Radiationless decay processes

A simple model has been developed to describe multiphonon decay processes in weakly coupled systems and this has been found to give a good fit to experimental data obtained on trivalent rare-earth ions in solids.[9] For decay across an energy gap ΔE by the emission of p phonons of energy $\hbar\omega$ ($p=\Delta E/\hbar\omega$), the nonradiative decay rate is given by

$$W_{\rm nr}^p(T)=W(0)\{\exp(\hbar\omega/kT)/[\exp(\hbar\omega/kT)-1]^p\ , \qquad (15)$$

where

$$W(0)=C\exp(-\alpha\Delta E)\ . \qquad (16)$$

Here, C and α are parameters involving the electron-phonon—interaction strength and the transition matrix elements. For many cases they have been found to be constants for f-f transitions of different trivalent rare-earth ions in a specific host and the spontaneous phonon-emission rate $W(0)$ shows a simple exponential dependence on the energy gaps of the various transitions.

Zverev *et al.*[10] have investigated radiationless relaxation processes of trivalent rare-earth ions in YAG (including the $^4G_{7/2}$-$^2G_{7/2}$ transition of Nd^{3+}) and found the results to obey the exponential energy-gap law with the parameters $C=9.7\times10^7$ s^{-1} and $\alpha=3.1\times10^{-3}$ cm. Temperature-dependent measurements were fitted with an effective phonon energy of 700 cm^{-1}, which is somewhat less than the maximum phonon energy in YAG crystals of 860 cm^{-1}.[11] This is consistent with other phonon effects on the optical spectra[1] and may be due to the fact that the highest-energy phonons are vibrations of AlO_4 groups which are less strongly coupled to the rare-earth ions than lower-energy lattice phonons.[11,12] Using these values for C, α, and $\hbar\omega$ in Eqs. (15) and (16) along with the appropriate energy gaps, the room-temperature radiationless decay rates for the $^2(F2)_{5/2}$ and $^2P_{3/2}$ metastable states can be calculated. In the former case, $\Delta E_3=3400$ cm^{-1} and $W_{\rm nr}^p(300\ {\rm K})=3.05\times10^3$ s^{-1}, while in the latter case, $\Delta E_2=2150$ cm^{-1} and $W_{\rm nr}^p(300\ {\rm K})=1.38\times10^5$ s^{-1}.

The calculated value of the nonradiative decay rate can be combined with the measured fluorescence decay rate to find the radiative decay rate of a metastable state through $\tau_f^{-1}=\beta^r+W_{\rm nr}^p$. The quantum efficiency of the level is then given by $\eta=\beta^r/\beta_f$. Applying this analysis to the two upper metastable states of Nd^{3+} ions in YAG gives the results listed as theoretical predictions in Table I. For the $^2(F2)_{5/2}$ level the result agrees quite closely with that obtained from fitting the time-resolved spectroscopy results using the simple rate-equation model discussed in the preceding sections. The value found here of $\eta_3=1.0$ for this level is significantly greater than the value of 0.21 estimated in Ref. 2 using a Judd-Olfelt calculation and absorption spectral data. Since the fluorescence transitions from this metastable state are not the same as the absorption transitions to the level, it is not surprising that this type of analysis does not give an accurate result. The value obtained for the nonradiative decay rate of the $^2P_{3/2}$ level can be combined with the measured fluorescence decay rates and the value of K' found from fitting Eq. (13) to experimental data to give the branching ratios for this metastable state as listed in Table I.

Nonradiative decay rates for $5d$-$4f$ transitions of trivalent rare-earth ions in YAG crystals have been measured in cases where $5d$ fluorescence can be observed.[12] Since no $5d$ fluorescence can be observed for Nd^{3+} ions, it has been concluded that the nonradiative decay rates must be very much faster than 10^7 s^{-1}, which is consistent with the value measured in this study. It should be noted that if the simple model of Eqs. (15) and (16) is employed with the values of C and α given above and $5d$-$4f$ energy gap of about 1800 cm^{-1} from Ref. 2, a significantly smaller nonradiative decay rate is predicted than the observed value. This is not surprising since the values of C and α are expected to be constant only for similar f-f transitions. The matrix elements for the d-f transitions will be significantly greater and should lead to predicted values closer to the observed rate. Performing similar measurements on other YAG samples with different rare-earth ions is necessary to determine values of C and α for $5d$-$4f$ transitions and checking the validity of the simple nonradiative decay model for these types of transitions.

C. Two-photon absorption cross sections

The theory of two-photon absorption applied specifically to trivalent rare-earth ions in solids was developed by Apanasevich *et al.*[13] The general expression for the two-photon absorption cross section is

$$\sigma_{if}^{(2)}=(2\pi/\hbar)\,|\,A_{if}^{(2)}\,|^2\rho_f(E)(\hbar\omega_p)^2\,, \tag{17}$$

where ω_p is the photon frequency, $\rho_f(E)$ is the density of final states, and $A_{if}{}^{(2)}$ is the matrix element for the transition. The density of final states is given by

$$\rho_f(E)=(\hbar\gamma_{if}/\pi)/[(\hbar\gamma_{if})^2+(\hbar\omega_{if}-2\hbar\omega_p)^2]\,, \tag{18}$$

where γ_{if} is the half-width of the final state. The major problem in the application of two-photon absorption theories is deciding how to treat the sum over intermediate states in the matrix element for the transition. Apanasevich *et al.*[13] chose the $5d$ levels as the intermediate states and derived an expression for the matrix element of the transition given by

$$|\,A_{if}^{(2)}\,|^2=(\hbar/\pi 2n)[(n^2+2)/3]^2[e^2/(mc^2)]^2[(me^4)^4/(8\pi^3c^2\hbar^4)](0.069)$$
$$\times\langle\alpha_f J_f||U^{(2)}||\alpha_i J_i\rangle^2(2J+1)^{-1}\left[\sum_k \langle 4f\,|\,r\,|\,5d_k\rangle^2/[(\hbar\omega_{ik}-\hbar\omega_p)-i\hbar\gamma_{ik}]\right]^2, \tag{19}$$

where γ_{ik} is the half-width of the intermediate state and $\langle\alpha_f J_f||U^{(2)}||\alpha_i J_i\rangle$ is the reduced matrix element of the tensor operator $U^{(2)}$ between the initial and final levels of the $4f$ configuration. The latter have been tabulated for the transitions of interest here.[14] The development of Ref. 13 neglects one-photon resonances and evaluates the sum over intermediate states in Eq. (17) by using an integral over hydrogenlike wave functions. Using their approach along with observed spectral information to estimate the density of final states, the two-photon absorption cross section for 532-nm pumping of the $^2(F2)_{5/2}$ level is evaluated from Eq. (17) to be 1.64×10^{-56} cm^{4}s/(photon ion). Considering the rough approximations involved in obtaining this theoretical estimate, the predicted value for the two-photon absorption cross section is very close to that derived from time-resolved spectroscopy data.

Obtaining a theoretical estimate for the two-photon absorption cross section for 354.7-nm pumping is more difficult since the nature of the final state of the transition is unknown. If it is assumed to be $5d$ level and the sum over intermediate states includes both $4f$ and $5d$ levels, the predicted value for $\sigma_2^{(2)}$ is found to be over 10 orders of magnitude smaller than the observed value. However, it is known that additional $4f$ levels exist in the high-energy region of the $5d$ bands,[2] and if one of these is assumed to be the final state of the two-photon transition, the calculation can proceed as described above giving the result $\sigma_2^{(2)}=1.11\times10^{-56}$ cm^{4}s/(photon ion). This is much closer to the observed value, but still significantly different indicating the inadequacy of the current theoretical model to treat this specific case.

Both of the two-photon absorption cross sections measured in this work involve real, resonant intermediate states. An unsuccessful attempt was also made to excite fluorescence of Nd^{3+} ions in YAG crystals from the fundamental emission of the Nd-YAG laser at 1060 nm. In this case there is no real, resonant intermediate state for a two-photon transition. Such excitation has been used for Nd^{3+} ions in other crystals.[15] The fact that no excitation could be achieved with the primary laser output at higher powers than used with the various harmonics shows the importance of the enhancement achieved with a real intermediate state. The multiphoton excitation spectra in Ref. 2 also exhibited enhancements at real intermediate state resonances. The theory of Ref. 12 used here does not account for the effects of single-photon resonances with intermediate $4f$ levels. However, models for evaluating the matrix elements using two sequential $4f$-$4f$ transitions or a $4f$-$4f$ transition followed by a $4f$-$5d$ transition predict theoretical values for the cross sections many orders of magnitude smaller than the experimentally observed values. It appears that the difference in magnitude of the two types of two-photon cross sections measured here is associated with the factors of photon energy and density of final states in Eq. (17), not with differences in the transition matrix elements. It is important to note that the values of $\sigma^{(2)}$ reported here are much smaller than those that can generally be measured by transmission experiments.[16]

D. Conclusions

In summary, the use of high-power, picosecond laser excitation of Nd^{3+} ions in YAG crystals has provided new information about the excited-state dynamics of this system. These results have practical applications with regard to pumping Nd-YAG lasers as well as fundamental interest in the areas of multiphoton absorption and radiationless relaxation processes. The time-resolved spectroscopy technique provides a very sensitive way to characterize the properties of different metastable states of a system and to quantitatively determine two-photon absorption cross sections and $5d$-$4f$ radiationless decay rates.

ACKNOWLEDGMENTS

This work was sponsored by the U.S. Army Research Office and by the National Science Foundation under Grant No. DMR-82-16551.

*Permanent address: Physics Department, Central State University, Edmond, OK 74008.

[1]R. C. Powell, in *Nd-YAG Lasers,* edited by L. G. DeShazer (Springer, Berlin, 1984).
[2]M. A. Kramer and R. W. Boyd, Phys. Rev. B **23**, 986 (1981).
[3]A. Niklas and W. Jelenski, Phys. Status Solidi A **77**, 393, (1983).
[4]N. S. Rooze and N. A. Anisimov, Opt. Spectrosc. **38**, 356 (1975).
[5]R. C. Powell, D. P. Neikirk, and D. Sardar, J. Opt. Soc. Am. **70**, 486 (1980).
[6]W. F. Krupke, IEEE J. Quantum Electron. **QE-7**, 153 (1971).
[7]B. DiBartolo, *Optical Interactions in Solids* (Wiley, New York, 1968).
[8]D. J. Robbins and P. J. Dean, Adv. Phys. **27**, 499 (1977).
[9]L. A. Riseberg and M. J. Weber, Prog. Opt. **14**, 89 (1977).
[10]G. M. Zverev, G. Ya. Kolodnyi, and A. M. Onishchenko, Zh. Eksp. Teor. Fiz. **60**, 920 (1971) [Sov. Phys.—JETP **33**, 497 (1971)].
[11]G. A. Slack, D. W. Oliver, R. M. Chrenko, and S. Roberts, Phys. Rev. **177**, 1308 (1969).
[12]M. J. Weber, Solid State Commun. **12**, 741 (1973).
[13]P. A. Apanasevich, R. I. Gintoft, V. S. Korolkov, A. G. Makhanek, and G. A. Skripko, Phys. Status Solidi B **58**, 745 (1973).
[14]W. T. Carnall, P. R. Fields, and K. Rajnak, J. Chem. Phys. **49**, 4424 (1968).
[15]S. Singh and J. E. Geusic, in *Optical Properties of Ions in Crystals,* edited by H. M. Crosswhite and H. W. Moos (Interscience, New York, 1967), p. 493.
[16]M. Ito and N. Mikami, Appl. Spectrosc. Rev. **16**, 299 (1980).